A&A 370, 265–272 (2001)
DOI: 10.1051/0004-6361:20010137

Astronomy & Astrophysics

The supernova remnants G 67.7+1.8, G 31.5–0.6 and G 49.2–0.7

F. Mavromatakis[1], J. Papamastorakis[1,2], J. Ventura[1,2,3], W. Becker[3], E. V. Paleologou[2], and D. Schaudel[3]

[1] University of Crete, Physics Department, PO Box 2208, 710 03 Heraklion, Crete, Greece
[2] Foundation for Research and Technology-Hellas, PO Box 1527, 711 10 Heraklion, Crete, Greece
[3] Max-Planck Institut für extraterrestrische Physik, Giessenbachstrasse, 85740 Garching, Germany

Received 20 November 2000 / Accepted 12 January 2001

Abstract. Optical CCD imaging and spectroscopic observations of three supernova remnants have been performed for the first time. Filamentary and diffuse emission is discovered from the supernova remnant G 67.7+1.8 located $\sim$82′ to the south of CTB 80's pulsar. The Hα and sulfur emission are almost equally strong at a level of $\sim$20 10^{-17} erg s^{-1} cm^{-2} arcsec^{-2} suggesting shock–heated emission. Electron densities less than 240 cm^{-3} are estimated, while the weak [O III] emission suggests shock velocities in the range of 60–80 km s^{-1}. Emission can also be seen in the ROSAT All Sky Survey data which indicate an extended hard X-ray source. Emission from G 31.5–0.6 is detected only in the Hα + [N II] image at a typical flux level of 35 10^{-17} erg s^{-1} cm^{-2} arcsec^{-2}. The morphology of the observed radiation is diffuse and partially correlated with the non–thermal radio emission. Deep long–slit spectra detect sulfur line emission which is not strong enough to identify it as emission from shocked gas. Finally, optical emission from G 49.2–0.7 is obscured by several dark nebulae which probably give rise to significant X-ray attenuation. The Hα + [N II] flux is typically $\sim$40 10^{-17} erg s^{-1} cm^{-2} arcsec^{-2} while the [S II] flux is very weak, not allowing its identification as shock–heated. However, a small area of $\sim 3' \times 1'$ emits strong sulfur flux relative to Hα ([S II]/H$\alpha \sim 0.6$). This area is located in the south–east of G 49.2–0.7, close to the outer boundaries of the X–ray and radio emission. However, deep optical spectra would be required to firmly establish the nature of this emission and its association to G 49.2–0.7.

Key words. ISM: general – ISM: supernova remnants – ISM: individual objects: G 67.7+1.8, G 31.5–0.6, G 49.2–0.7

1. Introduction

Most supernova remnants have been discovered by their non–thermal synchrotron radio emission and their shell morphology. Optical observations may detect light from a remnant depending on the distance and age of the remnant, and the properties of the local interstellar medium. The interstellar medium is not homogeneous or uniform, encompassing denser regions of interstellar "clouds". It is the interaction of these clouds with the primary shock wave of a middle aged remnant that ultimately gives rise to optical radiation. Imaging observations of supernova remnants use interference filters to isolate main optical emission lines like Hα 6563 Å, Hβ 4861 Å, [S II] 6716, 6731 Å and [O III] 5007 Å. The [S II] to Hα ratio serves as a discriminator between H II and shock–heated emission, although in limiting cases supplementary data on the target should be sought (e.g. Fesen et al. 1985). Information about the amount of interstellar extinction can be extracted from the Hα to Hβ ratio while possible variations of this ratio over the remnant's extent may indicate interaction with the local interstellar medium (e.g. Osterbrock 1989). Provided that the [O III]5007 Å line is observed in a remnant, its intensity relative to Hβ can provide valuable information about the shock speed (e.g. Cox & Raymond 1985). Spectroscopic observations, on the other hand, offer the advantage of more detailed spectral information allowing for comparison with published shock models, but at the expense of spatial coverage.

In an effort to broaden our knowledge about the least observed supernova remnants, we performed optical observations of three known radio remnants that had not been detected before in optical wavelengths. The supernova remnant G 67.7+1.8 was first detected in a galactic plane radio survey at 327 MHz by Taylor et al. (1992) using the Westerbork Synthesis Radio Telescope. The authors proposed its identification as a supernova remnant based on its dual–arc morphology and spectral index of $\alpha = -0.5$ ($S_\nu \sim \nu^\alpha$). It is characterized by an angular diameter of $\sim$9′ and a flux at 1 GHz of $\sim$1.2 10^{-21} W m^{-2} Hz^{-1} sr^{-1} (Taylor et al. 1992). A search in the literature for references to X-ray or optical observations turned out negative (Neckel & Vehrenberg 1987). However, a careful examination of the red POSS plates reveals faint but

Send offprint requests to: F. Mavromatakis,
e-mail: fotis@physics.uoc.gr

filamentary emission along the north part of the shell of G 67.7+1.8, while diffuse X–ray emission is also seen in the ROSAT All Sky Survey data.

The shell–like morphology of the radio continuum emission at 4750 MHz of G 31.5–0.6 and the non–thermal emission led Fürst et al. (1987) to propose the identification of this object as a supernova remnant. The spectral index is found in the range of −0.2 to −0.5 with a flux density of ∼1.8 Jy at 4750 MHz. The POSS plates do not show any traces of optical emission that could be attributed to G 31.5–0.6, while the detection of X-ray emission is not reported in the literature. Case and Bhattacharya (1998) proposed a distance of 16.7 kpc to G 67.7+1.8 based on the Σ – D relation and a distance of 12.9 kpc to G 31.5–0.6.

The third target of our observations was the supernova remnant G 49.2–0.7. This remnant is also known as W51C because it belongs to the radio complex W51, including the H II regions W51A and W51B. The 330 MHz radio image of Subrahmanyan and Goss (1995) shows an extended structure of angular dimensions ∼50′ × 35′ while the ROSAT soft X–ray data also suggest a similar extent (Koo et al. 1995). The spectral analysis of the ROSAT data showed that a thermal model could account for the observed spectrum. Koo et al. (1995) quote a shock temperature of ∼3 10^6 K, a shock velocity of ∼500 km s^{-1} and an age of ∼30 000 yrs. The authors proposed that the remnant is located ∼6 kpc away.

In this work we present deep CCD images of the forementioned remnants in Hα + [N II], [S II], [O II] and [O III]. Information about the observations and the data reduction is given in Sect. 2. In Sect. 3–5 we present the results of our imaging observations. We also discuss the results from the long–slit spectra taken at specific locations of interest. Finally, in Sect. 6 we discuss the physical properties of G 67.7+1.8 and the implications of the current observations for the properties of G 31.5–0.6 and G 49.2–0.7.

2. Observations

2.1. Optical images

The observations presented here were performed with the 0.3 m telescope at the Skinakas Observatory. The fields of the radio remnants were observed in June 16, and July 08–11, 1999. Two different CCDs were used during the observations. The first was a 1024 × 1024 Thomson CCD which resulted in a 69′ × 69′ field of view and an image scale of 4″ per pixel. The second was a 1024 × 1024 Site CCD which had a larger pixel size resulting in a 89′ × 89′ field of view and an image scale of 5″ per pixel. The characteristics of the interference filters are listed in Table 1 while the number of frames taken in each filter is given in Table 2. The exposure time of a single frame was 1800 s. The final images in each filter are the average of the individual frames. All coordinates quoted in this work refer to epoch 2000. G 67.7+1.8 was also observed with the 1.3 m telescope at Skinakas Observatory on August 21, 2000. The object was imaged with the Hα + [N II] filter, is not flux calibrated and is characterized by a scale of 1″ per pixel.

Standard IRAF and MIDAS routines were used for the reduction of the data. Individual frames were bias subtracted and flat-field corrected using well exposed twilight flat-fields. The spectrophotometric standard stars HR 7596, HR 7950, HR 8634, and HR 718 were used for flux calibration.

Table 1. Interference filter characteristics

Filter	Wavelength[a] $(FWHM)$(Å)	Line (%) contributions
Hα +[NII]	6555 (75)	100, 100, 100[b]
[SII]	6708 (27)	100, 18[c]
[OII]	3727 (28)	100, 100[d]
[OIII]	5005 (28)	100
Cont red	6096 (134)	–
Cont blue	5470 (230)	–

[a] Wavelength at peak transmission for $f/3.2$.
[b] Contributions from λ6548, 6563, 6584 Å.
[c] Contributions from λ6716, 6731 Å.
[d] Contributions from λ3727, 3729 Å.

Table 2. Log of the exposure times

	Hα + [N II]	[S II]	[O III]	[O II]
G 31.5–0.6	5400[a](3)[b]	5400 (3)	1800(1)	1800(1)
G 49.2–0.7	7200(4)	7200(4)	1800(1)	1800(1)
G 67.7+1.8	3600(2)	3600(2)	3600(2)	3600(2)

[a] Total exposure times in s.
[b] Number of individual frames.

2.2. Optical spectra

Long–slit spectra were obtained on August 22 and 23, 2000 using the 1.3 m Ritchey–Cretien telescope at Skinakas Observatory. One long–slit spectrum of G 67.7+1.8 was obtained on July 18, 1999 and is flux calibrated. All other spectra are not flux calibrated. The spectrophotometric standard stars HR 718 and HR 7596 were used to determine the detector's sensitivity function. The data were taken with a 1300 line mm^{-1} grating and a 800 × 2000 Site CCD having a 15 μm pixel size which resulted in a 1.04 Å pixel^{-1}. The slit had a width of 7.″7 and, in all cases, was oriented in the south-north direction. The number of available spectra from each remnant and the exposure time of each spectrum are given in Table 3.

3. The supernova remnant G 67.7+1.8

3.1. The Hα + [N II] and [S II] line emission

The supernova remnant G 67.7+1.8 appears as a ∼9′ long and ∼10″ wide filament in the Hα+[N II] and [S II] images,

Table 3. Spectral log

G 67.7+1.8	G 31.5–0.6	G 49.2–0.7	GAL 67.58+1.88
3[a]	2	3	1
3600[b] s	2700 s	2400 s	2400

[a] Number of spectra collected.
[b] Exposure time of individual spectra.

Table 4. Typically measured fluxes

	G 67.7+1.8	G 31.5–0.6	G 49.2–0.7
Hα + [N II]	40	35	30
[S II]	20	< 6	5
[O III]	2	< 10	< 5
[O II]	3	< 6	< 6

Fluxes in units of 10^{-17} erg s^{-1} cm^{-2} arcsec^{-2}.

oriented in the SW to the NE direction (Fig. 1). Diffuse emission to the south of the filament is present but still within the boundaries of the radio emission. In Table 4 we list typical fluxes measured in the calibrated images of the observed remnants. In cases where we failed to detect emission in a specific filter, the 3σ upper limit is quoted. The Hα + [N II] image also shows a small scale, diffuse structure $\sim$12.′3 to the SW of the G 67.7+1.8, at $\alpha \simeq 19^{\rm h}53^{\rm m}57^{\rm s}$ and $\delta \simeq 31°21'54''$ (Fig. 2). This structure has a typical extent of $\sim$3.′3 and emits Hα + [N II] radiation at a level of $\sim$20–35 10^{-17} erg s^{-1} cm^{-2} arcsec^{-2}. It is probably unrelated to G 67.7+1.8 since the detected emission is well outside the faintest radio contours. A single 2400 s long–slit spectrum was obtained from this object, and the results are given in Table 5. We designate this source as GAL 67.58+1.88 since it was not previously catalogued.

3.2. The [O III] and [O II] images

The filament first seen in Hα+[N II] is also detected in the oxygen forbidden lines of 5007 Å and 3727 Å (images not shown here) but the emission is quite weak. Continuum subtraction and a light smoothing on the resulting images were necessary in order to clearly identify the filament. The overall length of the filament in [O III] is $\sim 8'$, however, the emission is not spatially continuous but two gaps are present. Interestingly, GAL 67.58+1.88 is also seen in these filters. It possesses a patchy appearance in the [O III] filter while the [O II] emission looks like an arc convex to the south. We estimate an [O III] flux of $\sim$3 10^{-17} erg s^{-1} cm^{-2} arcsec^{-2} and an [O II] flux of $\sim$5 10^{-17} erg s^{-1} cm^{-2} arcsec^{-2} for this new source.

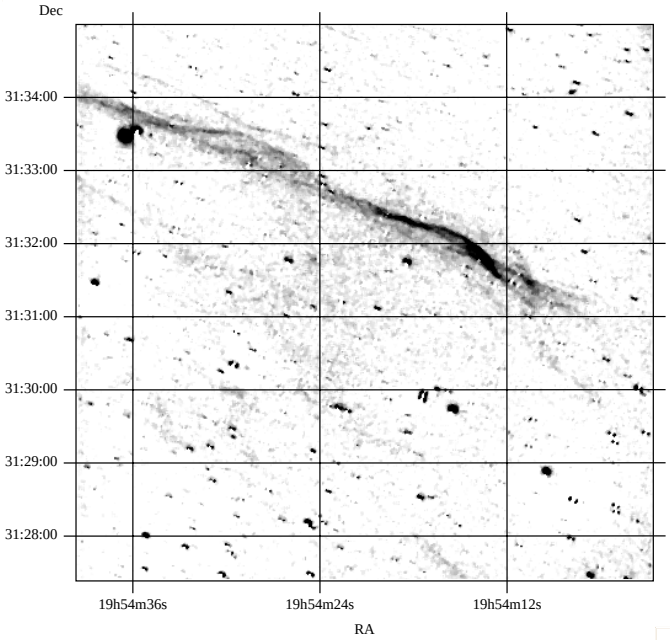

Fig. 1. G 67.7+1.8 imaged in the Hα+[N II] filter for 300 s with the 1.3 m telescope. The image has been smoothed to suppress the residuals from the imperfect continuum subtraction. Here and in the following images north is up, east to the left and the coordinates refer to epoch 2000

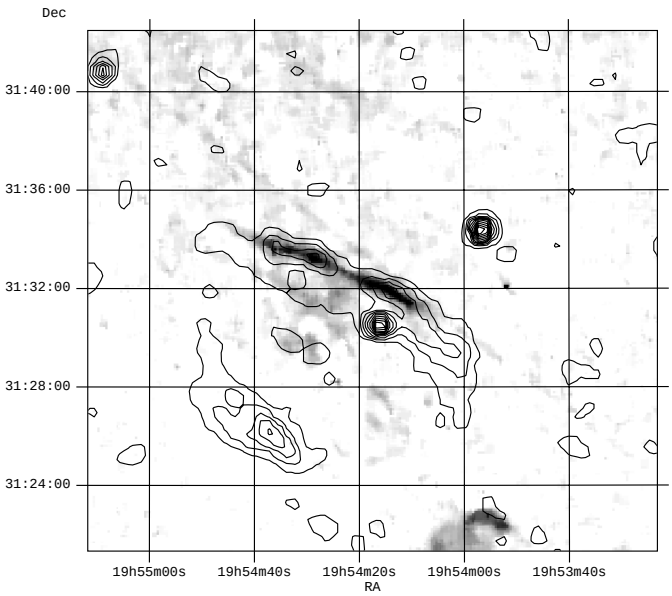

Fig. 2. The radio 1400 MHz contours (Condon et al. 1994) of G 67.7+1.8 overlaid to the Hα + [N II] image. The radio contours scale from 8 10^{-4} to 0.02 Jy/beam. The image has been smoothed to suppress the residuals from the imperfect continuum subtraction

3.3. The G 67.7+1.8 low resolution spectrum

The spectrum taken from G 67.7+1.8 (Table 5) shows optical radiation originating from shocked gas, since we estimate [S II]/Hα $\sim$ 1.2 ($\pm$ 0.1) and the optical filament is well correlated with the 1400 MHz and 4850 MHz radio data (Condon et al. 1994, Fig. 2). The sulfur line ratio of

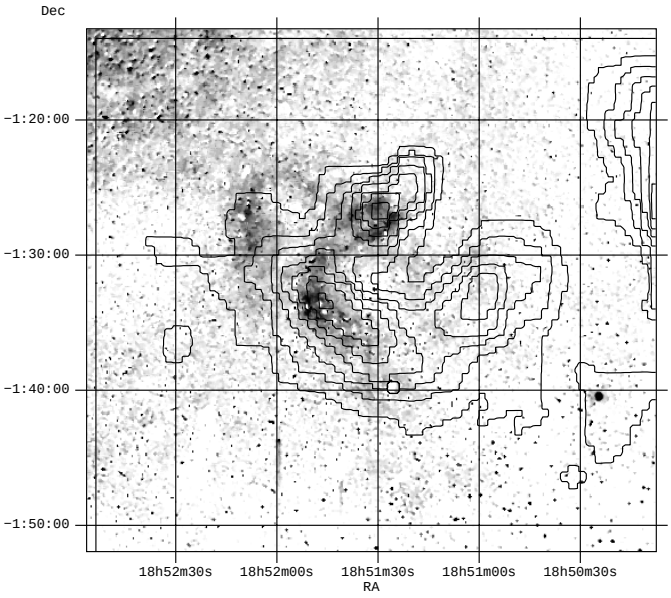

Fig. 3. The neighborhood around G 31.5–0.6 in the Hα+[N II] filter. The original image is $70' \times 70'$ and has been smoothed to suppress the residuals from the imperfect continuum subtraction. Shadings run linearly from 0.0 to 50 10^{-17} erg s^{-1} cm^{-2} arcsec^{-2} while the 4850 MHz radio contours (Condon et al. 1994) scale also linearly from 0.02 Jy/beam to 0.30 Jy/beam

1.28 ($\pm$ 0.08) suggests a low electron density $\sim$142 cm^{-3}, though taking the statistical error into account implies that densities in the range of 60–240 cm^{-3} would be compatible with our measurement. Finally, the Hβ flux is rather low compared to the Hα flux suggesting significant interstellar extinction (Hα/Hβ $\sim$ 10.9 $\pm$ 2.6).

The spectrum of GAL 67.58+1.88 does not allow a reliable determination of the nature of this object due to the large errors in the sulfur lines. However, the strong [N II] lines would suggest a circumstellar origin of the extended emission.

3.4. The ROSAT all–sky survey data

In the course of the ROSAT all-sky survey, G 67.7+1.8 was in the PSPC field of view between Oct. 22–25, 1990 for a total exposure time of $\sim$530 s. About 73 events were detected above the background level, in a circular area of $8'$ radius, at energies higher than 0.5 keV. No emission is seen above the background below 0.5 keV. The counts detected above 0.5 keV imply a surface brightness of $\sim$6.9($\pm$1.4) 10^{-4} cts s^{-1} arcmin^{-2}. According to Dickey & Lockman (1990), the galactic absorption along the line of sight is 10^{22} cm^{-2}. Assuming a thermal bremsstrahlung spectrum and fixing $N_{\rm H}$ to values in the range of 0.5–1.0 10^{22} cm^{-2}, we find temperatures of 0.2–0.3 keV, equivalent to blast wave speeds in the range of $\sim$400–500 km s^{-1}. A thermal blackbody spectrum requires lower temperatures of the order of $\sim$0.15 keV. The low number of detected photons do not allow us to uniquely identify the nature of the X–ray emission. According to the NVSS data, three faint radio sources appear close to the center of G 67.7+1.8 which could be indicative of emission from a young neutron star. Lorimer et al. (1998) searched for radio emission from a pulsar in the area of G 67.7+1.8 using the Jodrell Bank Radio facility. No radio pulsar was detected down to a level of 0.8 mJy.

4. The supernova remnant G 31.5–0.6

The radio contours at 4850 MHz (Condon et al. 1994), plotted linearly from 0.02 Jy/beam to 0.30 Jy/beam, are overlaid with our Hα + [N II] image (Fig. 3). The correlation of the optical and radio data may suggest their physical association, although the lack of strong [S II] emission makes this identification very difficult. The observed optical emission appears as a broad incomplete shell of diffuse emission convex to the NW. Typical Hα+[N II] fluxes and the 3σ upper limits on the [S II], [O II] and [O III] fluxes are given in Table 4.

4.1. The spectrum of G 31.5–0.6

The analysis of the optical images showed that strong Hα + [N II] emission is present to the south–east and north–west areas. However, the latter area of emission coincides with the location of an elongated small diameter source (GAL 31.650–00.649) reported by Fürst et al. (1987) which is characterized by a flat radio spectrum. Consequently, the slit was placed at the former area where non–thermal emission was detected and at a right ascension of $18^{\rm h}51^{\rm m}49^{\rm s}$ and a declination of $-1°34'20''$. The spectra taken in this area show that the Hα emission is stronger than the sulfur emission (Table 5).

5. The supernova remnant G 49.2–0.7

The supernova remnant G 49.2–0.7 lies close to the galactic plane along with several H II regions as well as with dark nebulae being projected on it (Fig. 4). A search in the SIMBAD database resulted in $\sim$25 H II regions within a circular field of 1° diameter. However, only three H II regions overlap W51C and these are GAL 049.2-00.7, GAL 049.0-00.6 (Wilson et al. 1970) and SH 2–79 (Acker et al. 1983). The observed optical emission occupies an angular extent of $\sim 40' \times 40'$ and the morphology in the Hα+[N II] and [S II] filters is diffuse. The observed radiation seems to split into two parts separated by a dark lane of material running along $\alpha \simeq 19^{\rm h}22^{\rm m}50^{\rm s}$. The east part shows several patches of emission in Hα + [N II] while the west part appears more diffuse. The sulfur line flux is relatively weak and thus, the image is not shown here. Optical diffuse or filamentary emission from the G 49.2–0.7 area is not detected in our [O II] and [O III] images (Table 4). The diffuse emission observed to the north–west of the dark lane may be associated with W51B. The optical emission west of this lane and south of $13°55'$ is probably not related to W51B but even its relation to W51C is not

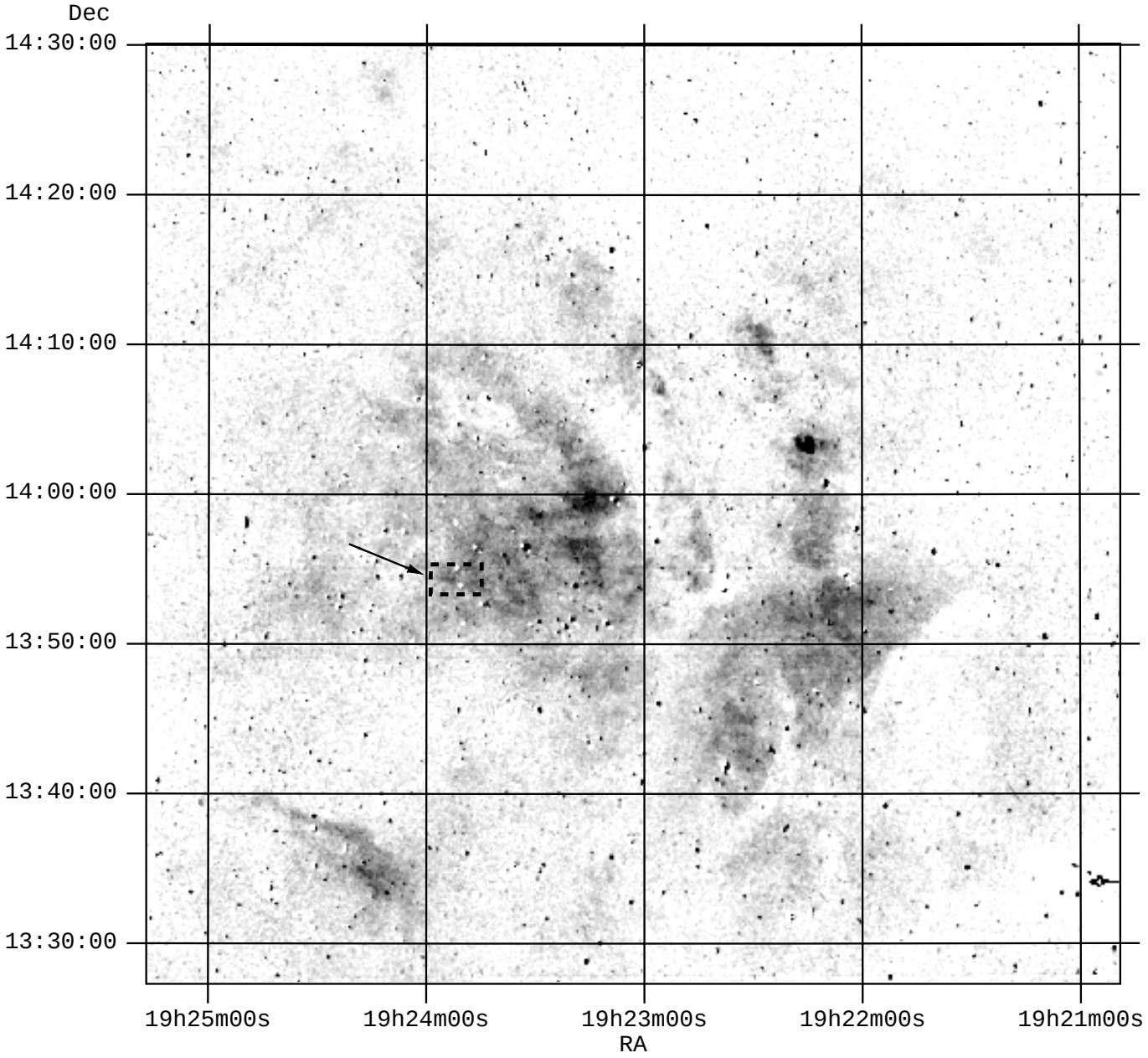

Fig. 4. The supernova remnant G 49.2–0.7 (W51C) imaged in the Hα+[N II] filter. The image has been smoothed to suppress the residuals from the imperfect continuum subtraction and the shadings run linearly from 0.0 to 50 10^{-17} erg s^{-1} cm^{-2} arcsec^{-2}. The arrow points to the area where enhanced [S II] emission is detected

clear since it is located outside the main body of the radio emission of W51C. However, some radio contours at 330 MHz (Subrahmanyan & Goss 1995) do overlap this optical emission.

5.1. The optical spectrum of G 49.2–0.7

The slit was placed at a bright spot of the diffuse emission seen in the east, in the Hα + [N II] image, which coincides with the area of radio emission from the remnant W51C. The area west of $\sim 19^{\rm h}23^{\rm m}$ is mainly dominated by W51B which is an H II region. The slit was placed at $\alpha = 19^{\rm h}23^{\rm m}09^{\rm s}$ and $\delta = 13^{\circ}59'39''$ and the signal to noise weighted average fluxes of the detected lines are shown in Table 5, where it is seen that the sulfur emission is weak relative to the Hα.

6. Discussion

The supernova remnants G 67.7+1.8 and G 31.5–0.6 are among the least observed remnants both in radio and optical wavelengths. This is not true for G 49.2–0.7 where extended radio and X–ray observations have revealed its physical properties.

Table 5. Relative line fluxes

	G 67.7+1.8	G 67.58+1.88	G 31.5–0.6	G 49.2–0.7
Line (Å)	$F^{a,b}$	$F^{a,b}$	$F^{a,b}$	$F^{a,b}$
4861 Hβ	92 (24)[c]	< 516	< 85	< 100
5007 [OIII]	89 (26)	641 (25)	–	–
6300 [O I]	283 (8)	–	–	–
6360 [O I]	98 (21)	–	–	–
6548 [N II]	192 (11)	777(21)	144 (16)	118 (16)
6563 Hα	1000 (3)	1000 (17)	1000 (3)	1000 (2)
6584 [N II]	631 (4)	2368 (8)	444 (25)	400 (5)
6716 [S II]	647 (4)	246 (59)	159 (12)	137 (12)
6731 [S II]	506 (5)	144 (83)	116 (15)	99 (18)
Hα/Hβ	10.9 (24)	> 1.94	> 11.8	> 10
[S II]/Hα	1.15 (4)	0.40 (50)	0.27 (10)	0.24 (10)
$F(6716)/F(6731)$	1.3 (6)	–	1.4 (19)	1.4 (22)

[a] Uncorrected for interstellar extinction.
[b] Listed fluxes are a signal to noise weighted average of the available spectra.
[c] Numbers in parentheses represent the relative (%) error of the quoted fluxes.
All fluxes normalized to $F(\mathrm{H}\alpha) = 1000$.

6.1. The G 67.7+1.8 radio remnant

The radio remnant G 67.7+1.8 is detected for the first time in the optical band as well as in the soft X–ray band by ROSAT. Both the positional correlation and the nature of the optical spectrum provide convincing evidence that the observed emission is indeed associated with G 67.7+1.8. The long–slit spectra suggest a low electron density ($\sim$140 cm^{-3}) but even the small (6%) error in the sulfur line ratio cannot exclude densities in the range of 60–240 cm^{-3}. The shock velocity is estimated to be less than 100 km s^{-1} given the weak [O III] emission and probably will lie in the range of 60–80 km s^{-1} (Cox & Raymond 1985; Hartigan et al. 1987) while the strong sulfur emission relative to Hα suggests a partially neutral medium. In order to obtain a better insight to the properties of G 67.7+1.8, a reliable distance determination is necessary. However, given the limited number of available observations, the Σ–D relation is the only tool available for this purpose. Case & Bhattacharya (1998) quote a distance of 16.7 kpc but the large errors on the proportionality factor and the exponent of the Σ–D relation allow a wide range of distances from $\sim$7–27 kpc. In view of the optical observations reported here, distances less than $\sim$17 kpc are more probable, otherwise detection of optical radiation would be very difficult due to interstellar extinction. The Hα/Hβ ratio of $\sim$11 corresponds to an interstellar extinction of 1.7 ($\pm$0.3) and thus supports distances much lower than 17 kpc (Hakkila et al. 1997, see also Mavromatakis et al. 2000). Another approach to estimate distance would involve the measured electron density and assumptions about the shock velocity and initial explosion energy. In the following, we will assume a shock velocity V_s of 70 km s^{-1}, and an explosion energy E in the range of 10^{50}–10^{51} ergs. An energy of 10^{51} ergs is considered as the typical energy released in a supernova explosion. With the aid of the relation

$$n_{[\mathrm{SII}]} \simeq 45\ n_\mathrm{c} \times (V_\mathrm{s}/100\ \mathrm{km\ s^{-1}})^2 \quad (1)$$

given by Fesen & Kirshner (1980), the above assumptions and the measured range of electron densities, we estimate that the preshock cloud densities n_c will lie in the range of 3–11 cm^{-3}. McKee & Cowie (1975) derived an equation relating the energy of explosion, shock radius and shocked cloud parameters as

$$E = 2\ 10^{46} \beta^{-1} n_\mathrm{c}\ (V_\mathrm{s}/100\ \mathrm{km\ s^{-1}})^2\ (r_\mathrm{s}/1\ \mathrm{pc})^3\ \ \mathrm{erg}, \quad (2)$$

where β is a factor of the order of 1–2, and r_s is the shock radius in pc. Using Eq. (2) and the range of preshock cloud densities, we find that for an explosion energy of 10^{50} erg the distance should lie in the range 7–12 kpc, while for an explosion energy of 10^{51} erg the distance should lie in the range of 16–26 kpc. These naive calculations show that the energy released during the supernova explosion must be significantly less than the canonical energy of 10^{51} erg. The soft X–ray data are equally well fitted by thermal bremsstrahlung or blackbody models and suggest temperatures in the range of 0.15–0.3 keV. However, the low counting statistics do not allow for a reliable determination of the column density, temperature and X–ray flux. Dedicated X–ray observations would be required to better understand the physical properties of G 67.7+1.8 and its surroundings.

A new source of diffuse emission is detected close to G 67.7+1.8, although not related to the remnant. The current observations suggest strong [O III], [N II], Hα but weak [S II] emission characteristic of emission of circumstellar origin. The bright blue star GSC 02669–04343 is

found at the west boundary of GAL 67.58+1.88 but it is not clear if they are related in any way. Higher resolution imaging and spectral observations would be needed to study this source in detail.

6.2. G 31.5–0.6, a source of weak sulfur line emission

A search in the SIMBAD database revealed several H II regions and dark nebulae within the field of G 31.5–0.6. The candidate supernova remnant GAL 31.7–1.0 (Gorham 1990) is located to the south–east of G 31.5–0.6 but we do not find any strong signs of optical emission. The Hα + [N II] emission from the vicinity of G 31.5–0.6 is diffuse with the H II region GAL 31.65–00.649 superposed on its north–west part. The positional correlation between the optical and radio data and their similar shapes would suggest the identification of the optical flux as emission from G 31.5–0.6, even though a chance superposition cannot be excluded. The lower limit on the Hα/Hβ ratio (>12) translates to a lower limit on the neutral hydrogen column density of 8 10^{21} cm^{-2} which is consistent with the column density of $\sim$1.3 10^{22} cm^{-2} given by Dickey & Lockman (1990). The ratio of the sulfur lines to Hα is 0.27, which is lower than the limit of $\sim$0.4 required to optically identify a supernova remnant. Although the fluxes of the sulfur lines are relatively accurately established (7–8σ), their line ratio is consistent with electron densities lower than $\sim$380 cm^{-3}. The low value of the [S II]/Hα ratio and the high value of the $F(6716)/F(6731)$ ratio are more suggestive of a spectrum of an H II region rather than of a SNR spectrum. Thus, the current data cannot identify the observed emission as emission from shocked gas, despite the positional correlation.

6.3. The complex around G 49.2–0.7

Extended optical emission is present in the Hα+[N II] filter from G 49.2–0.7, while it is substantially reduced in the [S II] filter. No optical emission, at our sensitivity threshold, is detected in both oxygen filters. Long–slit spectra obtained from the brighter areas seen in the Hα + [N II] filter do not suggest emission from shock–heated material. Both the [S II]/Hα and the sulfur lines ratio are indicative of H II emission (e.g. Fesen & Hurford 1995). It is possible that the emission within the slit was dominated by the H II region G 049.0–00.6 detected in an H 109α survey by Wilson et al. (1970), even though the authors state that due to the complexity of the region it is difficult to accurately measure the sizes and temperatures of these regions. Koo et al. (1995) have presented evidence for a fast–moving molecular gas which blocks our view to the west areas of W51 and may be responsible for the dark lane present in the optical data as well as in the X-ray data. The authors also found variations in the column density across the source of X-ray emission while the gas temperature remained essentially constant. Even though the [S II] emission is generally weak, a $\sim 3' \times 1'$ area seems to emit stronger sulfur flux at a level of $\sim$5 10^{-17} erg s^{-1} cm^{-2} arcsec^{-2}. The corresponding Hα + [N II] flux suggests that we may be observing emission from shocked gas since we estimate a [S II]/Hα ratio of $\sim$0.6. This region is located in the south–east boundary of the X-ray and radio emission and specifically, at a location of strong soft X–ray emission (Fig. 3a of Koo et al. 1995). The presence of H II regions, variable X-ray attenuation and molecular flows may render impossible the detection of shock–heated emission from G 49.2–0.7. Nevertheless, it is possible that certain areas in the south of G 49.2–0.7 suffer less absorption and some optical emission may escape the remnant unobscured. Long–slit spectra at the specified location should be able to determine unambiguously whether the detected emission is shock–heated or not.

7. Conclusions

Three poorly-known supernova remnants were observed and detected for the first time in the optical band. A thin long filament is detected in the north boundary of the radio emission from G 67.7+1.8. Its spatial correlation to the radio emission and the long–slit spectra suggest its identification as optical emission from a supernova remnant. A new faint structure called GAL 67.58+1.88 is detected to the south–west of G 67.7+1.8 but its nature is not yet clear. The imaging observations of G 31.5–0.6 detect Hα+[N II] emission which is found to be partially correlated with the radio emission. However, long–slit spectra show that the sulfur emission is not strong enough to justify shock–heated emission. Optical emission is detected from the area of G 49.2–0.7 in the Hα + [N II] filter while the measured fluxes in the [S II] filter are quite weak. A patch of $\sim 3' \times 1'$ in the south–east emits more [S II] flux than its surroundings. It could be possible that the south areas of G 49.2–0.7 suffer less absorption, allowing for the detection of shock–heated emission. However, the nature of the emitted radiation in the south–east would be uniquely identified only through deep, long–slit spectra.

Acknowledgements. We would like to thank the referee, R. A. Fesen, for his comments which helped to clarify certain issues of this work. Skinakas Observatory is a collaborative project of the University of Crete, the Foundation for Research and Technology-Hellas and the Max-Planck-Institut für Extraterrestrische Physik. This work has been supported by a P.EN.E.D. program of the General Secretariat of Research and Technology of Greece. J.V. acknowledges support through an Alexander von Humboldt Fellowship. This research has made use of data obtained through the High Energy Astrophysics Science Archive Research Center Online Service, provided by the NASA/Goddard Space Flight Center.

References

Acker, A., Marcout, J., Ochsenbeim, F., & Lortet, M. C. 1983, A&AS, 54, 315

Case, G. L., & Bhattacharya, D. 1998, ApJ, 504, 761

Clifton, T. R., Backer, D. C., Foster, R. S., et al. 1987, IAU Circ., No. 4422

Condon, J. J., Broderick, J. J., Seielstad, G. A., Douglas, K., & Gregory, P. C. 1994, AJ, 107, 1829
Cox, D. P., & Raymond, J. C. 1985, ApJ, 298, 651
Dickey, J. M., & Lockman, F. J. 1990, ARA&A, 28, 215
Fesen, R. A., & Kirshner, R. P. 1980, ApJ, 242, 1023
Fesen, R. A., Blair, W. P., & Kirshner, R. P. 1985, ApJ, 292, 29
Fesen, R. A., & Hurford, A. P. 1995, AJ, 110, 747
Fürst, E., Handa, T., Reich, W., Reich, P., & Sofue, Y. 1987, A&AS, 69, 403
Gorham, P. W. 1990, ApJ, 364, 187
Hartigan, P., Raymond, J., & Hartmann, L. 1987, ApJ, 316, 323
Hakkila, J., Myers, J. M., Stidham, B. J., & Hartmann, D. H. 1997, AJ, 114, 2043
Kaler, J. B. 1976, ApJS, 31, 517
Koo, B. C., Kim, K. T., & Seward, F. D. 1995, ApJ, 447, 211
Lorimer, D. R., Lyne, A. G., & Camilo, F. 1998, A&A, 331, 1002
Mavromatakis, F., Papamastorakis, J., Paleologou, E. V., & Ventura, J. 2000, A&A, 353, 371
McKee, C. F., & Cowie, L. 1975, ApJ, 195, 715
Neckel, T., & Vehreberg, H. 1987, Atlas of Galactic Nebulae, part II (Treugesell-Verlag)
Osterbrock, D. E. 1989, Astrophysics of gaseous nebulae (W. H. Freeman & Company)
Raymond, J. C., Hester, J. J., Cox, D., et al. 1988, ApJ, 324, 869
Subrahmanyan, R., & Goss, W. M. 1995, MNRAS, 275, 755
Taylor, J. H., Manchester, R. N., & Lyne, A. G. 1993, ApJS, 88, 529
Taylor, A. R., Wallace, B. J., & Goss, W. M. 1992, AJ, 103, 931
Whitford, A. 1958, AJ, 63, 201
Wilson, T. L., Mezger, P. G., Gardner, F. F., & Milne, D. K. 1970, A&A, 6, 364